

Finite Element Simulation and Prediction of Mechanical and Electrochemical Behavior on Crevice Corrosion in Sheet Pile Steel

Benamar Balegh^{a,*}, Habib Trouzine^b, Youcef Houmadi^c

^a Civil Eng Dep, Faculty of Technology, Sidi Bel Abbas University, Sidi Bel Abbas, Algeria

^b LGCE Civil Engineering and Environmental Laboratory, Sidi Bel Abbas University, Algeria.

^c SSL Smart Structures Laboratory, Ain Témouchent university center, Algeria

Received 24 June 2017

Accepted 21 June 2018

Abstract

A finite element method is proposed for modeling the crevice corrosion effect on sheet pile steel, through a multiphysics field coupling techniques. In this paper, the results show that while a tensile strain enhances stress uniformly through sheet pile steel, an increasing depth of crevice corrosion results in a concentrated stress at localized corrosion. When the crevice corrosion is under an elastic deformation, there is no apparent effect of mechanical–electrochemical interaction on corrosion. However, when the applied tensile strain on the side of crevice corrosion is enough to produce a plastic deformation, corrosion activity is also increasing.

© 2018 Jordan Journal of Mechanical and Industrial Engineering. All rights reserved

Keywords: Sheet pile steel; Mechano-electrochemical behaviour; modelling studies; Crevice corrosion.

1. Introduction

Corrosion of sheet pile steel is the term which is usually given to the level that is higher than expected corrosion loss. In an advanced state, typically after many years of exposure, this vertically oriented differential corrosion along the sheet pile length causes localized crevice of the wall thickness. Such crevice and loss of sheet pile wall thickness can have a significant effect on the structural capacity wherever the place of the crevice occurs. The general pattern of crevice corrosion is remarkable [1]. For U-profile sheet piling the perforations occur predominantly on the out-pans, while for Z-profile piles perforation appears to occur predominantly as elongated slots on the web of the Z shape as shown in Figure 1[2, 3]. In practice the corrosion rate is also assumed to be a linear function of time by most researchers [4] and the values on corrosion rates are recommended [5]. Corrosion behaviour of steel structural in soils, water, and air was studied with a specific conditions by means of several techniques also developed test method [6,7].

Many studies have mainly focused on the distribution of the electrical potential, current within the corrosion crevice, the mechanism and modeling of the phenomenon of cathodic protection [8,9]. Significant research has been performed in the past to understand the mechanisms of external corrosion of soil. Crevice with minimal overall metal loss of thickness can lead to the failure of structures

because of several corrosion types that can stem from pitting corrosion such as stress corrosion [10].

It has been recommended that mechanisms are there to describe the initiation of crevice corrosion which is attributable to the development of a differential aeration cell with the subsequent acidification of the crevice solution and/or migration of aggressive anions [11–13], there have been a number of industrial codes/standards, such as Eurocode 3 [5], that can be used to evaluate remaining strength and failure under complex stress/strain conditions. However, this industry code was developed according to corrosion process and grades of steel and environment of corrosion (air, soil, water). Besides, this model usually provide prediction of behavior steel structures at a relatively high tolerance as reported in literature [14,15].

The simulating parameters include stress distribution, corrosion potential, and current densities as a function of the corrosion crevice size and tensile strain. It is anticipated that this research provides a sufficiently reliable method for simulation and prediction of crevice corrosion on sheet pile steel under complex stress and strain conditions, and develop recommendations to industry for risk assessment[16, 17]

In this paper, a finite element model is developed to study the mechano-electrochemical effect of corrosion of a segment of sheet pile steel, under corrosion effects. The reliability of the model is validated by various mechanical, and corrosion measurements.

* Corresponding author e-mail: balegh.benamar@yahoo.com.

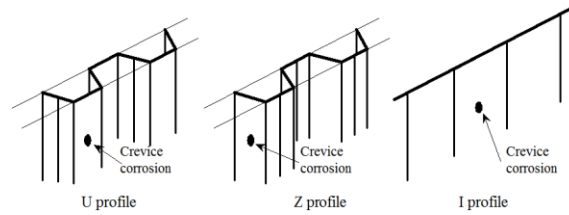


Figure 1: Sheet pile steel formed by U, Z and I profile piles and the types and locations of crevice corrosion.

2. Simulation

2.1. Boundary geometrical parameters

The simulation of mechano-electrochemical effect of corrosion of sheet pile steel was performed. The geometrical model containing crevice corrosion is shown in Figure 1, where the segment of sheet pile thickness is 18 mm and, the length is 60 mm for finite element simulation. The crevice corrosion on sheet pile wall is elliptically shaped, with a length of 2 mm, and its depths d_t are: 1 mm, 1.75 mm, 2.5 mm, 3.75 mm respectively. This work assumes an unchanged length with growing depth for crevice corrosion in order to investigate propagation of the corrosion defect along the sheet pile direction.

The boundary condition of solution is that the solution boundary is electrically isolated, except for the steel interface that is set as a free boundary at right side. While the bottom segment is fixed, the left segments loaded with prescribed tensile strains as described below and is set as an electric grounding. The mesh type used is triangular. A full mesh consists of 977 nodes with 133 edge elements and 18 integration points. The maximum and minimum element sizes are 1.6 mm and 0.001 mm, respectively, with a maximum element growth rate of 1.3 also the predefined size is extremely fine. A stationary solver of and time dependent solver is selected for this case.

The geometry of sheet pile segment is simplified into a 2D model due to the symmetrical property, as shown in Figure 2. The finite element simulation contains two aspects, mechanical elasto-plastic solid stress analysis of the steel sheet pile and corrosion secondary potential and current density analyses [18]

2.2. Simulation of mechanical parameters

An elasto-plastic solid stress simulation was performed on sheet pile steel. The isotropic hardening model is used, E is Young's modulus of 200 GPa. Von Mises yielding

criteria used for the elasto-plastic simulation then a stress is applied on the steel sheet pile along the longitudinal direction to simulate steel strain of 5 MPa [20]. The total strain ϵ is equal to the total deformation Δl divided by segment length l :

$$\epsilon = \frac{\Delta l}{l} \quad (1)$$

2.3. Simulation of electrochemical corrosion parameters

The interface of secondary corrosion, found under the electrochemistry corrosion, deformed geometry branch when adding a physics interface, describes the current and potential distributions in corrosion under the assumption that the variations in composition in the electrolyte are negligible [20]. The physics interface can be combined with physics interfaces modeling mass transport to describe concentration dependent current distributions.

The electrochemical reactions of iron dissolution occur in the crevice according to:

Anodic reaction :



which $\text{Fe}(s)$ is iron in solid state, $\text{Fe}^{2+}(\text{aq})$ is iron in liquid state and e is electron

Experimental polarization data is used for this reaction, where the local current density of the reaction is evaluated as:

$$i_{\text{Fe}} = f(\phi_s - \phi_l) \quad (3)$$

The crevice corrosion is modeled as a porous electrode, with the specific surface area, and the electric potential is assumed to be constant over the crevice, solving for electrostatic potential ϕ is disabled in the solver [21]. The problem is solved using a parametric sweep on a stationary solver, sweeping the potential in the electrode phase. The parametric sweep is needed to ensure that the intended active-to-passive polarization behavior is captured in the simulation, since due to the non-monotonic shape of the polarization curve the problem may have more than one solution. Several numerical models have been studied for describing crevice corrosion not only in the one-dimensional approximation, but also in the two and three-dimensional cases. In concentrated solutions in the presence of chemical reactions and practically with arbitrary boundary conditions as it is reported to describe crevice corrosion models [22, 23]. The FE simulation of mechano-electrochemical effect of crevice corrosion of sheet pile steel was performed using a commercial COMSOL Multiphysics [24].

Table 1: Composition of steel sheet piling used in study measured by Optical Emission Spectroscopy (wt%) [19]

Profile	C	P	Mn	si	S	Ni	Cr	Mo	Cu	Al	V	Ti	Sn	Pb	Fe
U	0.1	0.069	0.87	0.173	0.021	0.47	0.09	0.05	0.55	0.003	0.021	0.004	0.019	-	Bal.
Z	0.1	0.073	0.86	0.165	0.023	0.47	0.08	0.04	0.58	≤0.005	0.021	0.002	0.017	0.01	Bal.

3. Experimental testing

Specimens used in this paper were cut from a sheet of sheet pile steel wall along circumferential direction, with a chemical composition shown in Table 1. The specimen was machined into dumbbell shaped and its surface was ground up [25].

The test solution was a near-neutral pH bicarbonate solution, i.e., NS4 solution, which has been used widely to simulate electrolyte. The solution contained 0.483 g/L NaHCO₃, 0.122 g/L KCl, 0.181 g/L CaCl₂·H₂O and 0.131 g/L MgSO₄·7H₂O, and was made from analytic grade reagents and ultra-pure water at ambient temperature (22 °C).

The engineering stress-strain curve of sheet pile steel was obtained by tensile testing through a Bose Electroforce dynamic material test system. Potentiodynamic polarization curve was measured on steel electrode through a Solatron 1280° electrochemical workstation after a steady-state corrosion potential was achieved upon

immersing in NS4 solution for 1 h. The potential scanning rate was 0.3 mV/s, and potential polarization started at 0.9 V and ended at 0.6 V [26].

Mechanical properties of the steel and various electrochemical corrosion parameters derived from the polarization curve were used as initial conditions for FE. These included corrosion potential, corrosion current density.

4. Results and discussion

4.1. Von Mises stress under corrosion depth

Figure 4 shows the distributions of Von Mises stress at the crevice corrosion under various corrosion depths. It is seen that the local Von Mises stress level increases apparently and is distributed symmetrically to the center of the crevice that the highest stress occurs at the crevice center.

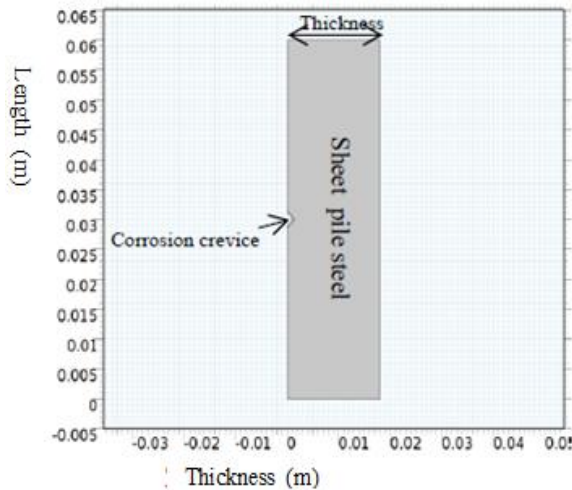


Figure 2: Geometry of model

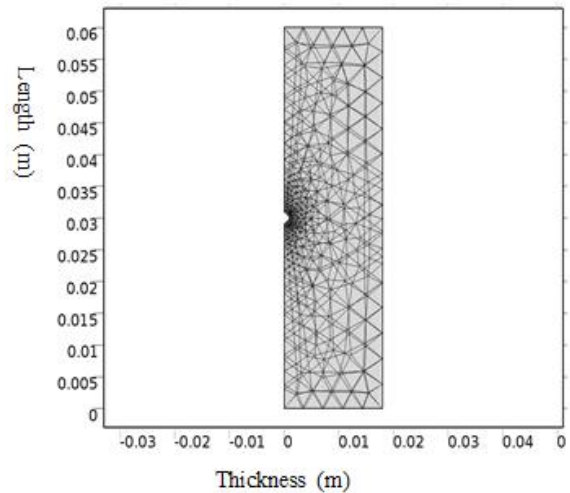


Figure 3: Meshing of model

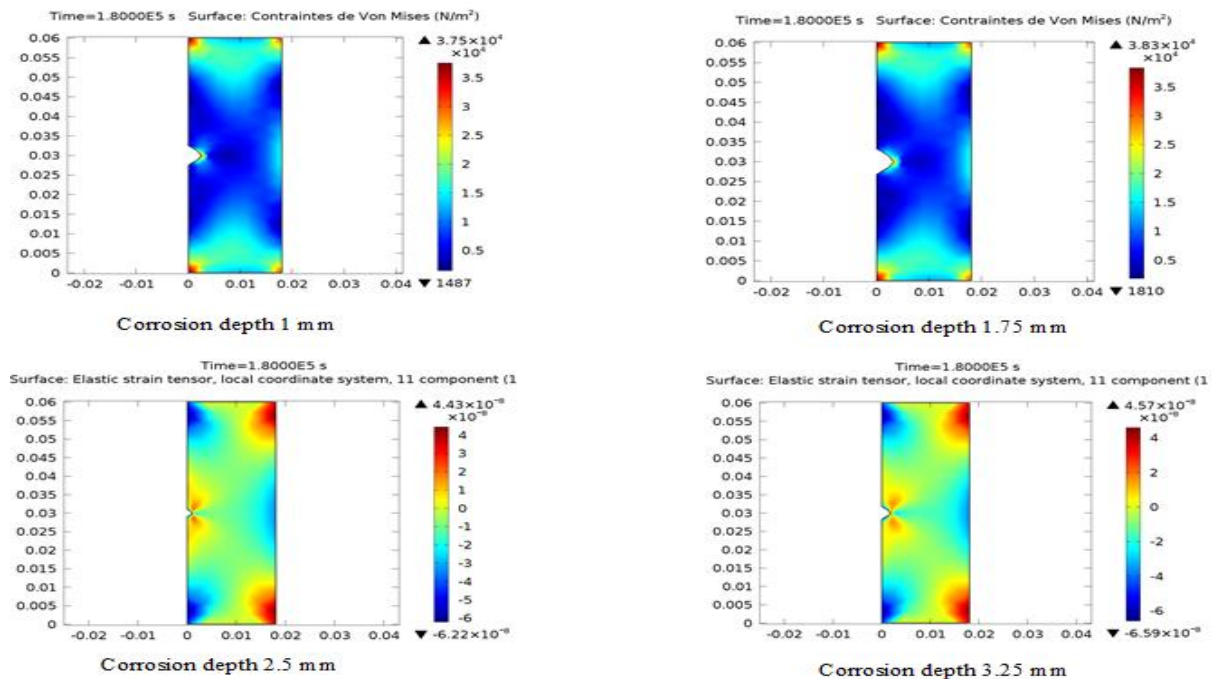


Figure 4: Distributions of Von Mises stress under various crevice corrosion.

4.2. Elastic strain under corrosion depth

Figure 5 shows the distributions of elastic strain tensor at the crevice corrosion under various corrosion depths. It is noticed, the local elastic strain level increases apparently at the opposite face of crevice corrosion as indicated by the red and dark red colors with minor change. It is seen that the strains is distributed symmetrically around the crevice that the highest stress locates at the center of crevice.

Figure 6 shows finite element simulating results of growth of von Mises stress values surrounding the crevice with increasing of depth corrosion in it. It is seen that the results obtained from simulation are well consistent with

the experimental data, indicating the validity and reliability of the finite element model. The von mises stress is further enhanced becomes apparent, as indicated by vectors pointing from the crevice center to the sides. The deeper of corrosion crevice results the higher stress concentration.

Figure 7 shows also growth of elastic strain values surrounding the crevice with increasing of depth corrosion in it. It is seen that the results obtained from simulation are well consistent with the experimental data, indicating the validity and reliability of the finite element model. The elastic strain is further enhanced. The deeper of corrosion crevice results the higher strain concentration.

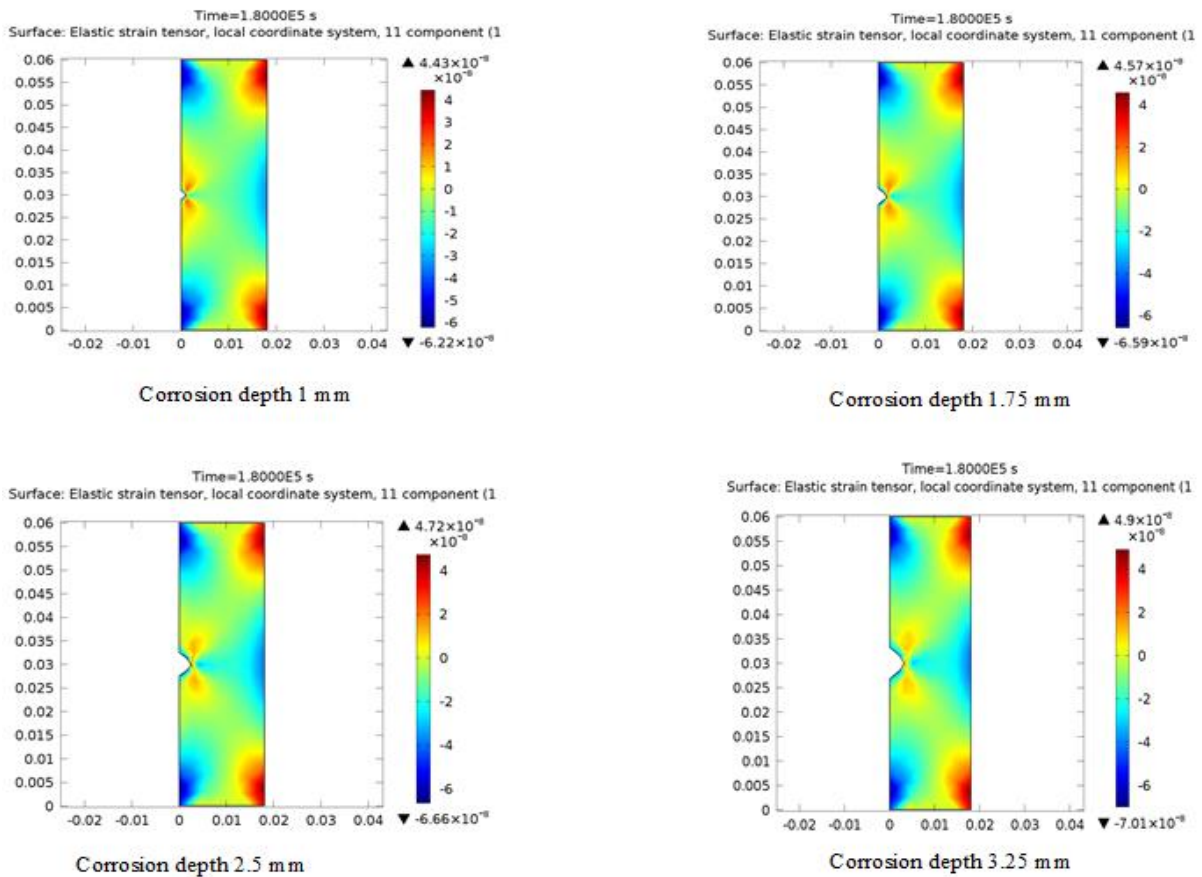


Figure 5: Distributions of elastic strain tensor under various crevice corrosion.

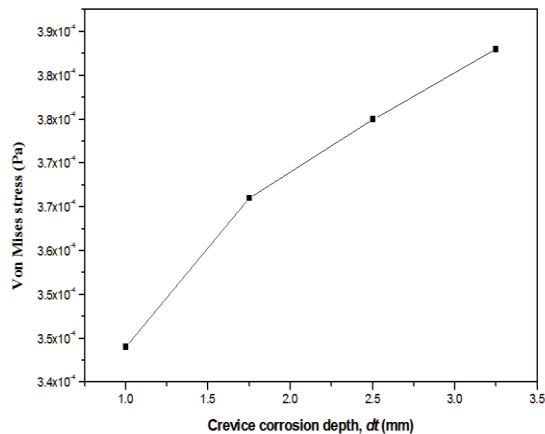


Figure 6: Linear distribution of von Mises stress along the bottom of crevice corrosion with various depths

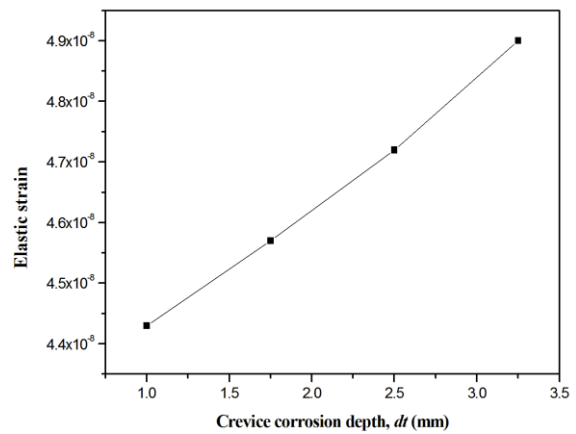


Figure 7: Linear distribution of elastic strain along the bottom of crevice corrosion with various depths.

4.3. Von Mises stress under load

Figure 8 shows the distributions of Von Mises stress at fixed depth corrosion of 1mm under various applied load represented in active forces which is naturally variant along of high of sheet pile steel. It is seen that, the local Von Mises stress level increases apparently, and also it is distributed symmetrically to the center of the crevice, that the highest stress occurs at the crevice center.

4.4. Elastic strain under load

Figure9 shows the distributions of elastic strain at the crevice corrosion under various applied load. The local elastic strain level increases apparently at the opposite face of crevice corrosion as indicated by the red and dark red colors.

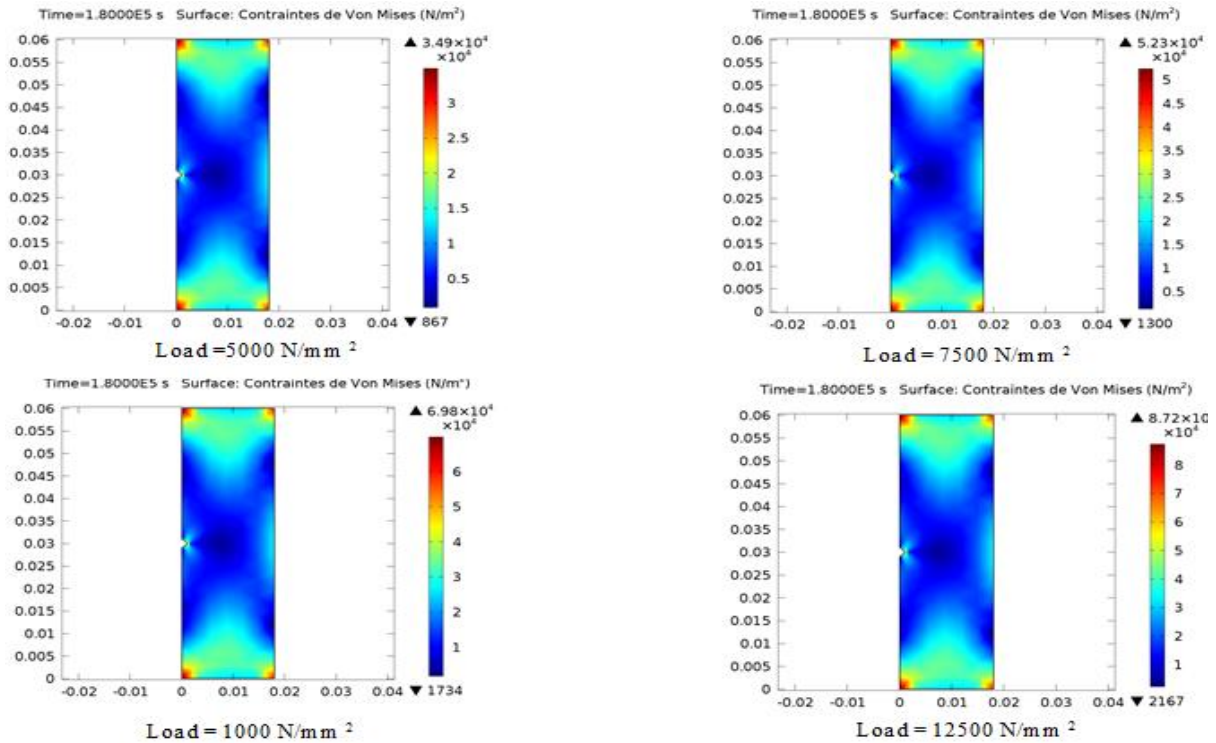


Figure 8: Distributions of von Mises stress at the corrosion crevice under various applied load.

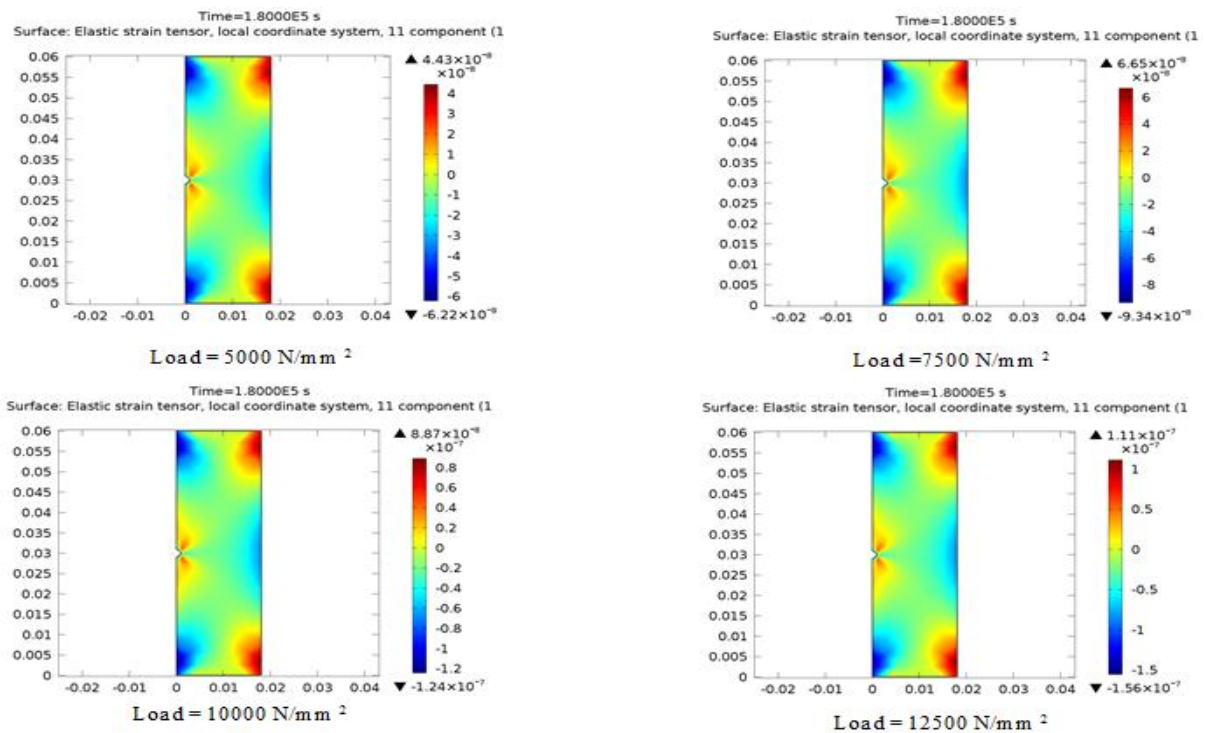


Figure 9: Distributions of elastic strain tensor at the corrosion crevice under various applied load.

Figures 10, 11 show finite element simulation results of growth of Von Mises stress and elastic strain values surrounding the corrosion crevice with increasing applied load. It is seen that the results obtained from simulation are well consistent, indicating the validity and reliability of the finite element model steel corrosion under mechanical-electrochemical interactions.

4.5. Electrolyte current density

Figure 12 shows the distributions of electrolyte current

density at the crevice corrosion under various corrosion depths. The local electrolyte current density level increases slightly at crevice corrosion as indicated by the red and dark red colors. It is seen that the electrolyte current density is distributed symmetrically to the center of the crevice, and the highest electrolyte current density occurs at the crevice center and the highest value 807 A/m^2 occurs at the small depth corrosion of 1mm, so there is inverse relationship between electrolyte current density and depth corrosion in steel.

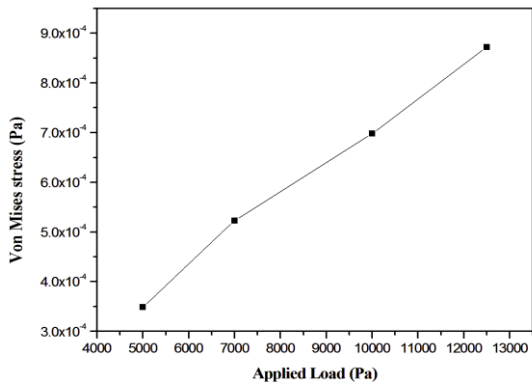


Figure 10: Linear distribution of von Mises stress along the bottom of crevice corrosion with various applied load.

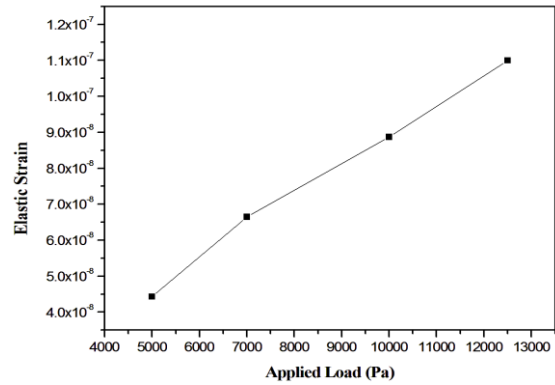
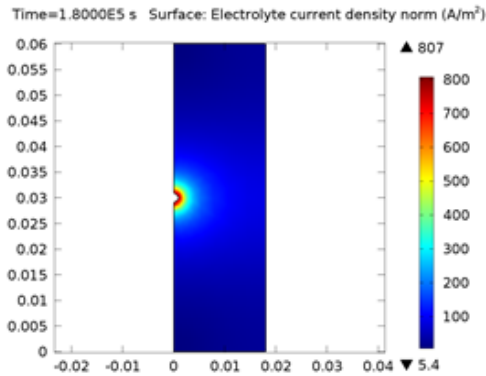
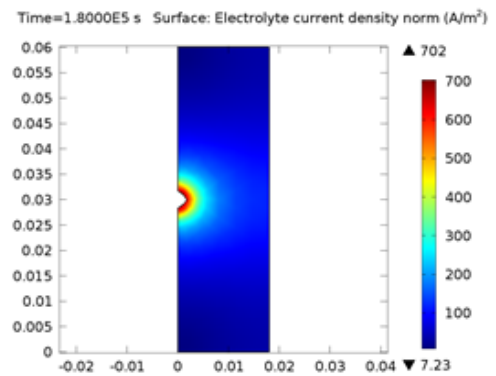


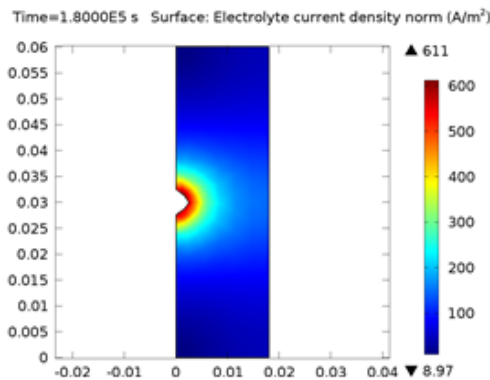
Figure 11: Linear distribution of elastic strain along the bottom of crevice corrosion with various applied load.



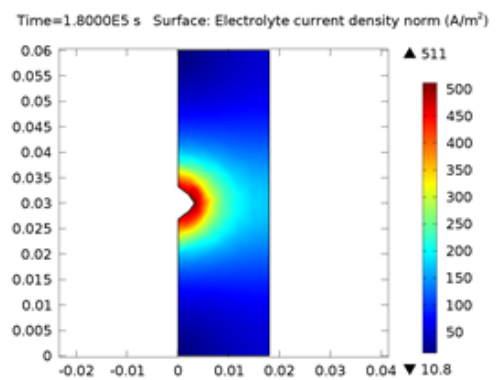
Corrosion depth 1 mm



Corrosion depth 1.75 mm



Corrosion depth 2.5 mm



Corrosion depth 3.75 mm

Figure 12: Distributions of electrolyte current density at the crevice corrosion.

4.6. Electrolyte potential

Figure 13 shows the distributions of electrolyte potential at the crevice corrosion under various corrosion depths. It is seen that, the local electrolyte potential level increases slightly at crevice corrosion as indicated by the red and dark red colors with minor change. While under growth of corrosion depth, it is recognized that the local electrolyte potential level increases remarkably surrounding the crevice corrosion as indicated by the red and dark red colors. It is seen that the electrolyte potential is distributed symmetrically to the center of the defect and the highest electrolyte potential occurs at the crevice center and the highest value 0.22 V occurs at the depth corrosion of 3.25 mm, so there is proportional relationship between electrolyte potential and depth corrosion in steel.

Figures 14, 15 show finite element simulating results of current density and corrosion potential of corroded sheet

pile steel model as a function of crevice corrosion depth, where the current density is decreased with crevice corrosion depth contrary what is concerning a corrosion potential which increase while a crevice corrosion is deepening.

Figures 16,17 show finite element simulating results of current density and corrosion potential of corroded sheet pile steel model as a function of Von Mises stress, where the current density is the sum of anodic and cathodic current densities which also decrease with Von Mises stress contrary what is concerning a corrosion potential which increase with Von Mises stress.

It is seen that the results obtained from FE simulation are well consistent with the experimental data, indicating the validity and reliability of the FE model in prediction of sheet pile steel corrosion under mechanical–electrochemical interactions.

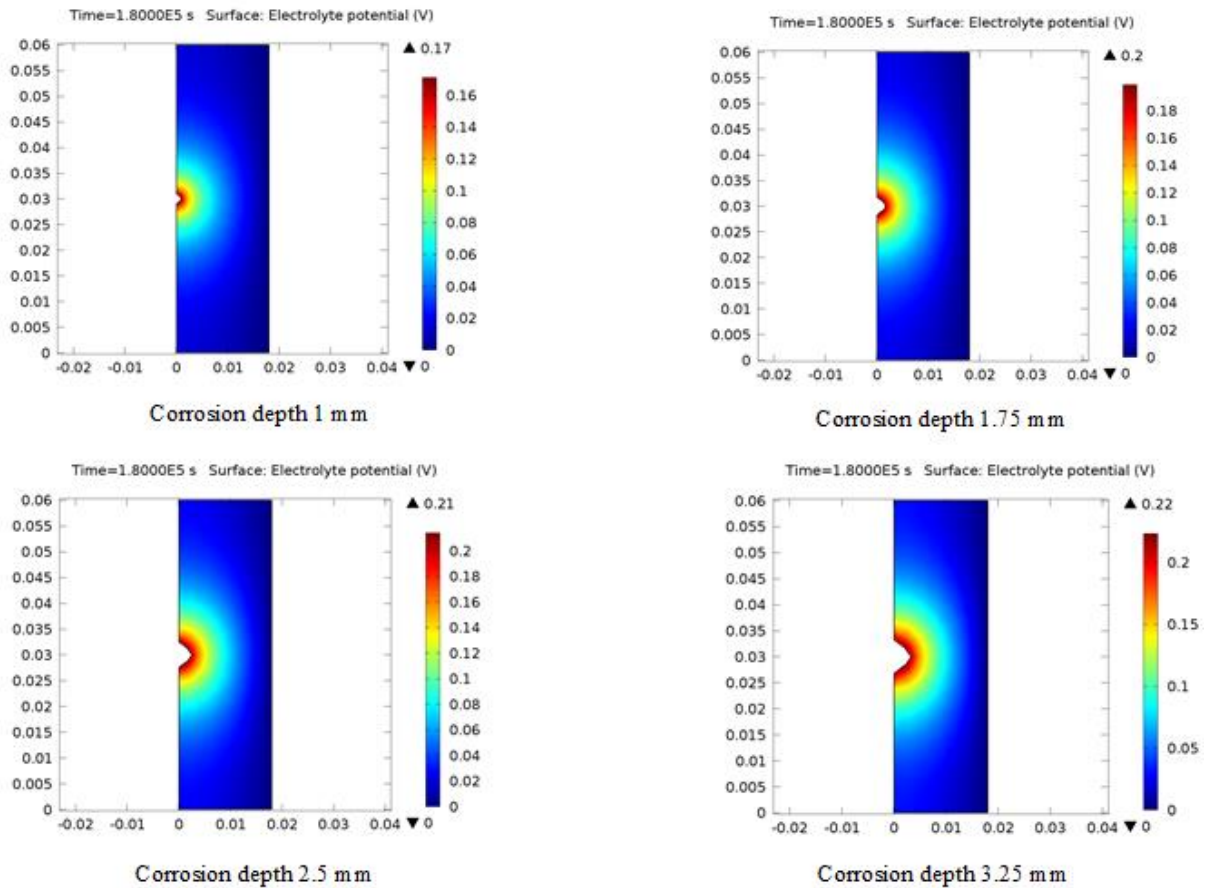


Figure 13: Distributions of electrolyte potential at the crevice corrosion.

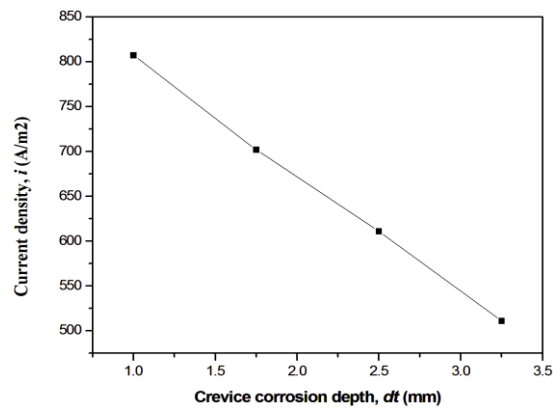


Figure 14: Linear distribution of current density along the bottom of crevice corrosion with various depth.

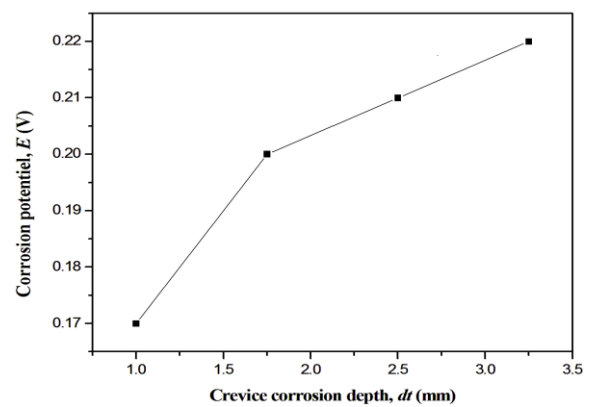


Figure 15: Linear distribution of corrosion potential along the bottom of crevice corrosion with various depth.

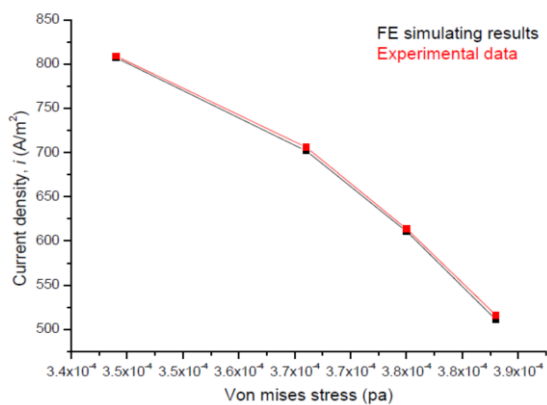


Figure 16: Linear distribution of Current density as a function of von Mises stress.

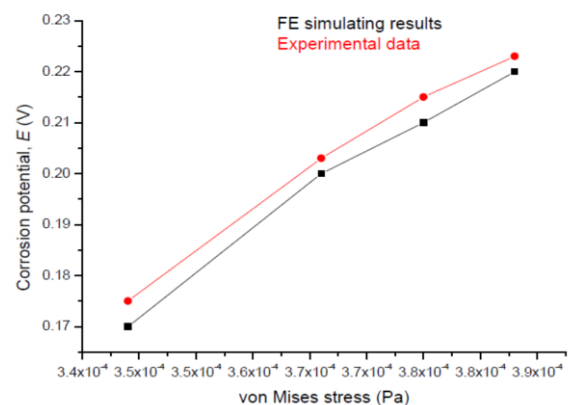


Figure 17: Linear distribution of corrosion potential as a function of von Mises stress.

5. Conclusions

- A finite element model is developed to study mechano-electrochemical effect of corrosion crevice at sheet pile steel through a multiphysics coupling simulation. The model enables simulation of the synergism of stress concentration and localized corrosion in sheet pile steel, moreover there is no comparison between present study and previous work.
- An increase of longitudinal tensile strain and depth of crevice corrosion enhance local stress on sheetpile steel, However, their effects on stress distribution are not similar. While a tensile elastic strain results in an overall enhancement of stress through the sheet pile steel, the increasing corrosion depth causes a more concentrated stress at the crevice center. Stress at side of the crevice actually decreases.
- When corrosion depth is under local elastic deformation, there is no apparent mechanical–electrochemical interaction affecting local corrosion. When elastic strain or the corrosion depth is further increased to result in a local plastic deformation, the local corrosion activity is increased remarkably.
- The region with a high stress, such as the crevice center serves as anode, and that under low stress, such as the sides of the corrosion crevice, as cathode. Anodic dissolution at the crevice center is further accelerated, while it is mitigated slightly on the sides of crevice. The

locally corrosion at the crevice center is further enhanced by the increasing depth of corrosion.

- An increasing depth of corrosion defect results in a concentrated stress at crevice corrosion. When the applied load on the side of geometry corrosion defect is sufficient to cause a plastic deformation at the crevice corrosion.

Acknowledgement

The research is supported by CNEPRU project. Our sincere thanks go to Civil Engineering & Environment Laboratory of Sidi Bel Abbes University and Smart Structures Laboratory at Ain Témouchent University Center, for the realization of this work.

References

- [1] H. Shu, F.M. Al-Faqeer, H.W. Pickering, Pitting on the crevice wall prior to crevice corrosion: Iron in sulfate/chromate solution, *Electrochimica Acta*. 56(2011)1719-1728.
- [2] E. Robert, A. Melchers, J. Robert, A. Jeffrey, M. Kayley, Localized corrosion of steel sheetpiling, *Corrosion Science*. 79 (2014)139-147.
- [3] I. Beech, S. Campbell, Accelerated low water corrosion of carbon steel in the presence of a biofilm harbouring sulphate-reducing and sulphur-oxidising bacteria recovered from a marine sediment, *Electrochimica Acta*. 54, 2008, 14-21.
- [4] H. Wall, L. Wadsö, Corrosion rate measurements in steel sheet pile walls in a marine environment, *Marine Structure*. 33 (2013)21-32.

- [5] European Committee for Standardization, Eurocode 3. Design of steel structures – part 5: piling, 2007
- [6] G. Palumbo, J. Banaś, A. Bałkowiec, J. Mizera, U. Lelek-Borkowska, Electrochemical study of the corrosion behaviour of carbon steel in fracturing fluid, *Journal of Solid State Electrochemistry*. 18 (2014)2933-2945.
- [7] E. Vannan, P. Vizhian, Corrosion Characteristics of Basalt Short Fiber Reinforced with Al-7075 Metal Matrix Composites, *Jordan Journal of Mechanical and Industrial Engineering*. 9 (2)2015,121-128.
- [8] F.M. Song, Predicting the chemistry corrosion potential and corrosion rate in a crevice formed between substrate steel and a disbonded permeable coating with a mouth, *Corrosion Science*. 55 (2012)107-115.
- [9] W. Sun, L. Wang, T. Wu, G. Liu, An arbitrary Lagrangian–Eulerian model for modelling the time-dependent evolution of crevice corrosion, *Corrosion Science*. 78 (2014)233-243.
- [10] A. Turnbull, D.A. Horner, B.J. Connolly, Challenges in modeling the evolution of stress corrosion cracks from pits, *Engineering Fracture Mechanics*. 76 (2009)633-640.
- [11] L.Y. Xu, Y.F. Cheng, Assessment of the complexity of stress/strain conditions of X100 steel pipeline and the effect on the steel corrosion and failure pressure prediction, in: *Proc. 9th International Pipeline Conference*, Calgary, Canada, (paper no. IPC2012-90087, 2012.
- [12] F.P. Ijsseling, Survey of Literature on Crevice Corrosion, (1979–1998), Report EFC 30, The Institute of Materials, London, 2000.
- [13] W.S. Tait, *An Introduction to Electrochemical Corrosion Testing for Practicing Engineers and Scientist*, 1st ed., PairODocs, Racine, WI, 1994.
- [14] P.O. Gartland, Modeling crevice corrosion for Fe Ni Cr Mo in chloride solutions, in: *12th International Corrosion Congress*, Houston, September, p. 1901, 1993
- [15] G.A. Zhang, Y.F. Cheng, Micro-electrochemical characterization of corrosion of pre-cracked X70 pipeline steel in a concentrated carbonate/bicarbonate solution, *Corrosion Science*. 52 (2010) 960–968.
- [16] Behrens D. *DECHEMA Corrosion Handbook, Corrosive agents and their interaction with materials, Chlorine Dioxide and Seawater*, 11,3-527-26662-3. Berlin ISBN, 1992.
- [17] L.Y. Xu, Y.F. Cheng, Reliability and failure pressure prediction of various grades of pipeline steel in the presence of corrosion defects and pre-strain, *International Journal of Pressure Vessels and Piping*. 89 (2012)75-84.
- [18] L.Y. Xu, Y.F. Cheng, Development of a finite element model for simulation and prediction of mechanochemical effect of pipeline corrosion, *Corrosion Science*. 73 (2013)150-160.
- [19] Gutman EM. *Mechanochemistry of Solid Surfaces*. World Scientific Publication, Singapore; 1994
- [20] G.R. Engelhardt, D.D. Macdonald, Possible distribution of potential and corrosion current density inside corroding crevices, *Electrochimica Acta*. 65 (2012)266- 274.
- [21] J.C Walton, *Mathematical Modeling of Mass Transport and Chemical Reaction in Crevice and Pitting Corrosion*, *Corrosion Science*. 30 (8/9)(1990)915-928.
- [22] Stewart K. *Crevice Corrosion by Cathodic Focusing*. PhD thesis, University of Virginia, 1999.
- [23] <http://www.virginia.edu/cese/research/crevicer.html>; 2002.
- [24] COMSOL Multiphysics, version 4.3, www.comsol.com.
- [25] L.Y. Xu, Y.F. Cheng, An experimental investigation of corrosion of X100 pipeline steel under uniaxial elastic stress in a near-neutral pH solution, *Corrosion Science*. 59 (2012)103–109.
- [26] L.Y. Xu, Y.F. Cheng, Corrosion of X100 pipeline steel under plastic strain in a neutral pH bicarbonate solution, *Corrosion Science*. 64 (2012) 145–152.